

Annulated tricyclic thiophenes and their photophysical properties

Elena V. Lukovskaya, Natalya V. Dyachenko, Andrey V. Khoroshutin,
Alla A. Bobyleva, Alexander V. Anisimov, Valentina A. Karnoukhova,
Gediminas Jonusauskas, Yurii V. Fedorov and Olga A. Fedorova

Table of Contents

1. Experimental Section.....	S1
1.1. Synthesis of 1 and 2	S2
1.2. ¹ H NMR Spectra, 2D NMR Spectra.....	S3
2. Photophysical properties.....	S11
2.1. Absorption and emission spectra.....	S11
2.2. Fluorescence decay curves	S13
2.3. Fluorescence quantum yield determination.....	S17
2.4. Quantum yields of <i>trans-cis</i> -isomerization	S17
References	S20

1. Experimental Section

All reagents and solvents (Acros, Aldrich, Merck) were used as purchased. ¹H and ¹³C NMR spectra were recorded on a Bruker Avance-400 and Bruker Avance-600 spectrometers (400.13 and 600.13 MHz frequencies for ¹H, 100 and 125 MHz for ¹³C) using CDCl₃ and CD₃CN as solvents and HMDS as internal standard. Chemical shifts were measured with 0.01 ppm accuracy, and coupling constants were determined with the accuracy to 0.1 Hz. For APT experiments, CH₂ and C chemical shifts are marked with asterisk.

For irradiation of samples, a 100 W low-pressure mercury lamp (AceGlass) was used, 70 mm arc length. The lamp was placed in a quartz immersion well (35 mm O.D.), which was inserted into a glass photoreactor with 45 mm I.D. The volume of the photoreactor was 100 ml, the irradiated solution volume was 65.5 ml; the thickness of the irradiated layer was 1 cm. Reaction mixture was stirred by argon bubbling coming from the cannula ended at the bottom of the reactor.

Fluorescence spectra were measured at 20±1 °C with a FluroLog-3-221 spectrofluorometer (Horiba Scientific) equipped with Time-Correlated Single Photon Counting (TCSPC) module and solid-state pulsed NanoLED emitting at 310 nm for fluorescence decay measurements. Melting points were measured with a Mel_temp II instrument and were not corrected. The reaction course and purity of isolated products were monitored by TLC on Kieselgel 60 F254 plates (Merck). Column chromatography was carried out on silica gel 0.060—0.200 mm (Acros). Elemental analyses were performed at the Laboratory of Organic Analysis of the Department of Chemistry of the M. V. Lomonosov Moscow State University. Electronic absorption spectra for kinetics measurements were recorded on spectrophotometer «Avantes AvaSpec-2048».

¹H and ¹³C (APT method) NMR spectra were recorded on a Bruker AVANCE-400 and Avance-500 spectrometers. Two-dimensional techniques HMQC, HMBC and COSY were used for the assignment of signals in the spectra. ESI mass spectra (ESI-MS) were acquired on an Agilent 1100 Series LC/MSD trap in the positive ion mode. Elemental analysis was performed in the A.N. Nesmeyanov Institute of Organoelement Compounds of Russian Academy of Sciences.

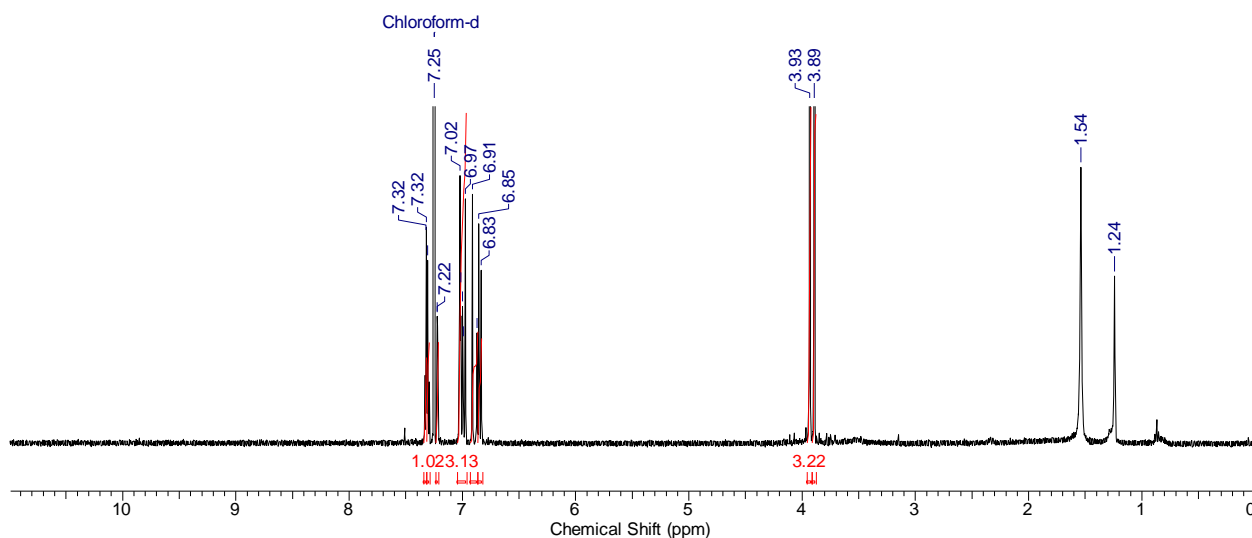
1.1. Synthesis of compounds 1 and 2.

3-[(E)-2-(3,4-Dimethoxyphenyl)ethenyl]thiophene (1) was synthesized according to the procedure reported for **2** [S1] from diethyl (3-thienylmethyl)phosphonate (1.0 g, 4.3 mmol) and 3,4-dimethoxybenzaldehyde (0.72 g, 4.3 mmol). The product was recrystallized from methanol, the yield was 0.86 g (3.3 mmol, 76%). The spectral data of **1** are identical to those reported in [S2], although it was synthesized differently.

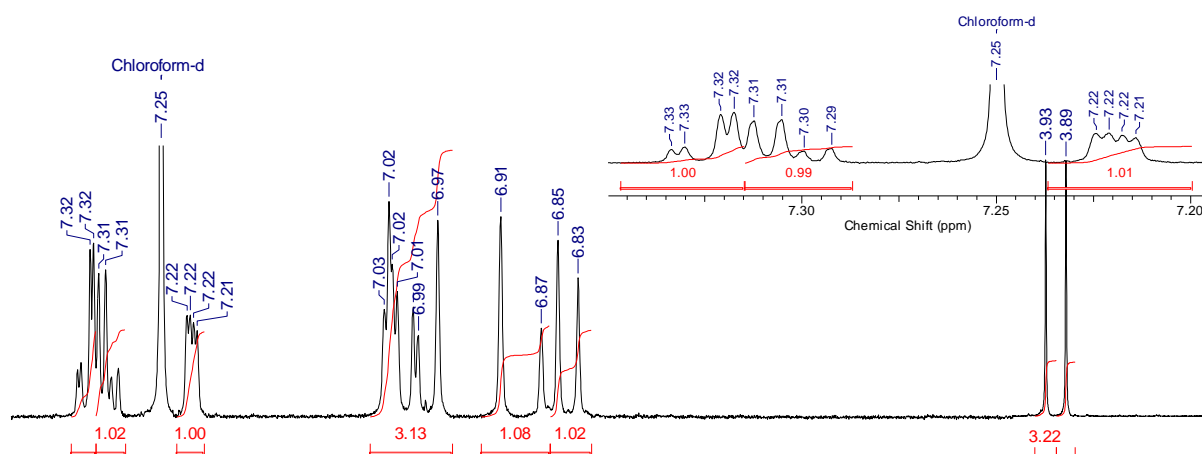
15-[(E)-2-(3-Thienyl)vinyl]-2,3,5,6,8,9,11,12-octahydro-1,4,7,10,13-benzopentaoxa-cyclopentadecane (2) was synthesized from 4-formylbenzo-15-crown-5 and diethyl-3-thienylmethyl phosphonate as reported [S1].

1.2. ^1H NMR Spectra, 2D NMR Spectra

a)



b)



c)

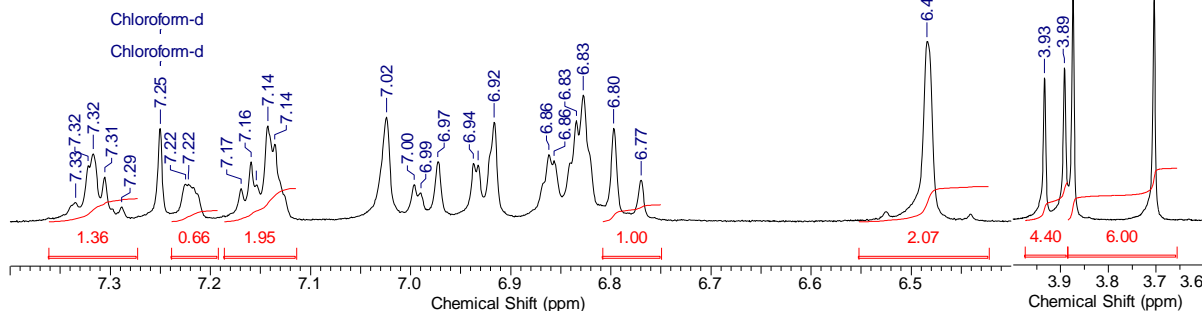


Figure S1. ^1H NMR of compound **1**. a) whole spectrum, b) aromatics & double bond and OCH_3 proton regions, c) the corresponding regions of *cis* and *trans*-isomers mixture after short irradiation time. Chemical shifts and coupling constants from the multiplets in the b, inset: 7.32, dd, $^3J=5.0, 1.4$; 7.30, dd, $^3J=5.0, 2.7$; 7.22, dd, $^3J=2.7, 1.4$.

1.2.1. Spectra of compound 2

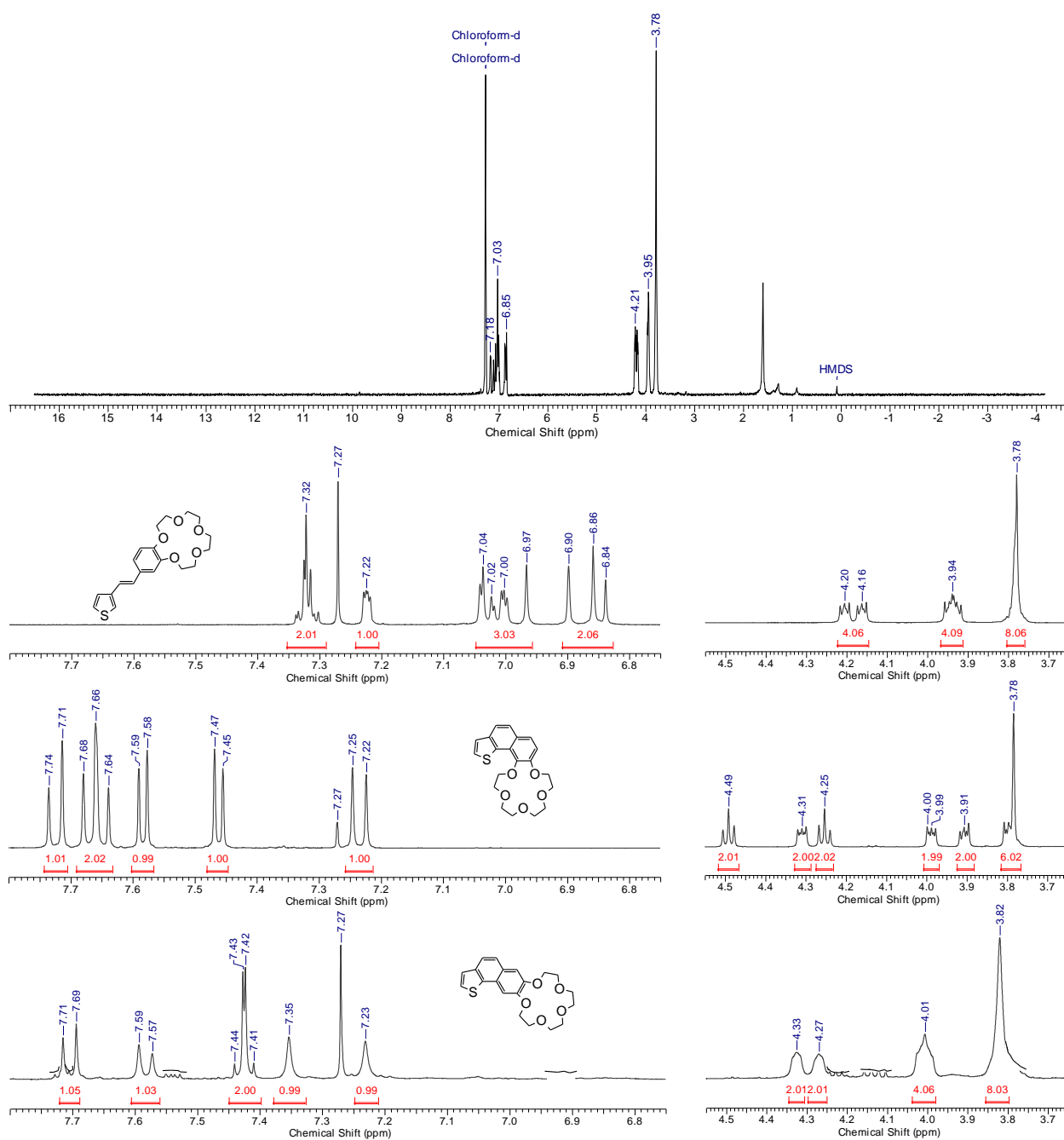


Figure S2. ^1H NMR-spectra of compound **2** and the comparison of its selected regions with those of the cyclized products, i.e. **4a,b** in CDCl_3 .

1.2.2. Spectra of compound 3b

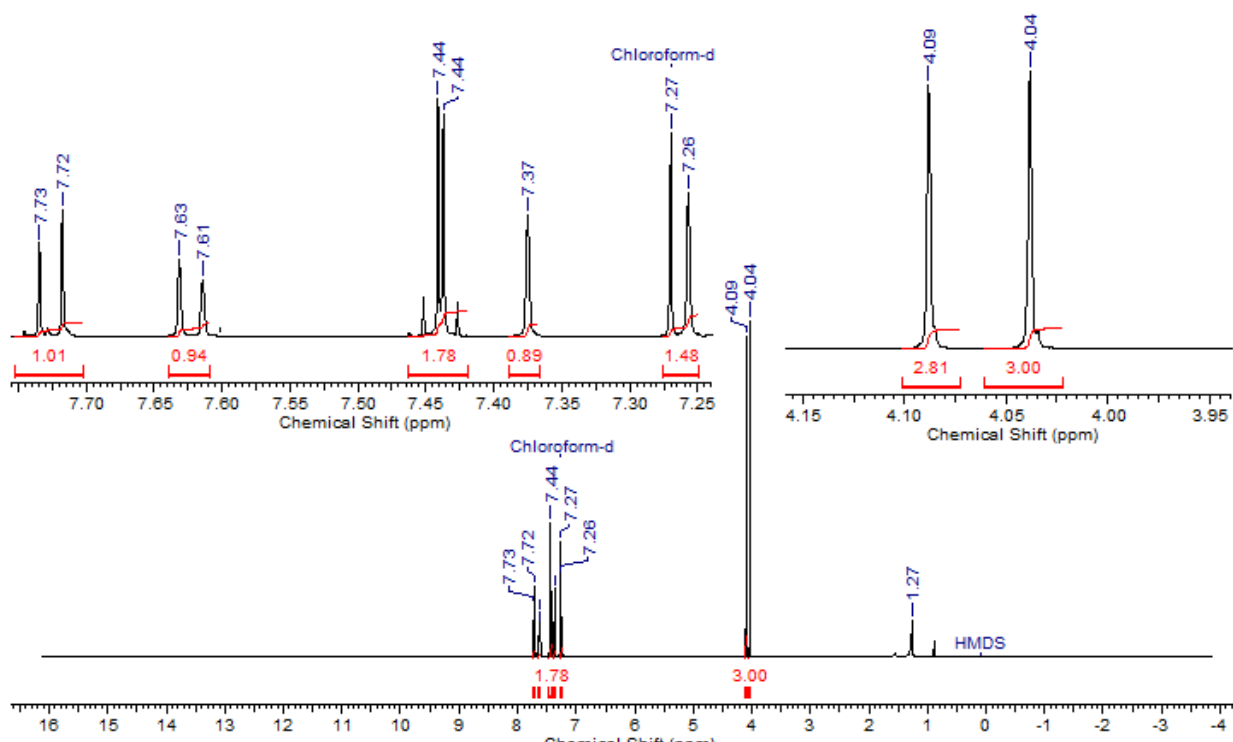


Figure S3. ¹H NMR-spectra of **3b** in CDCl₃, Bruker 500 MHz.

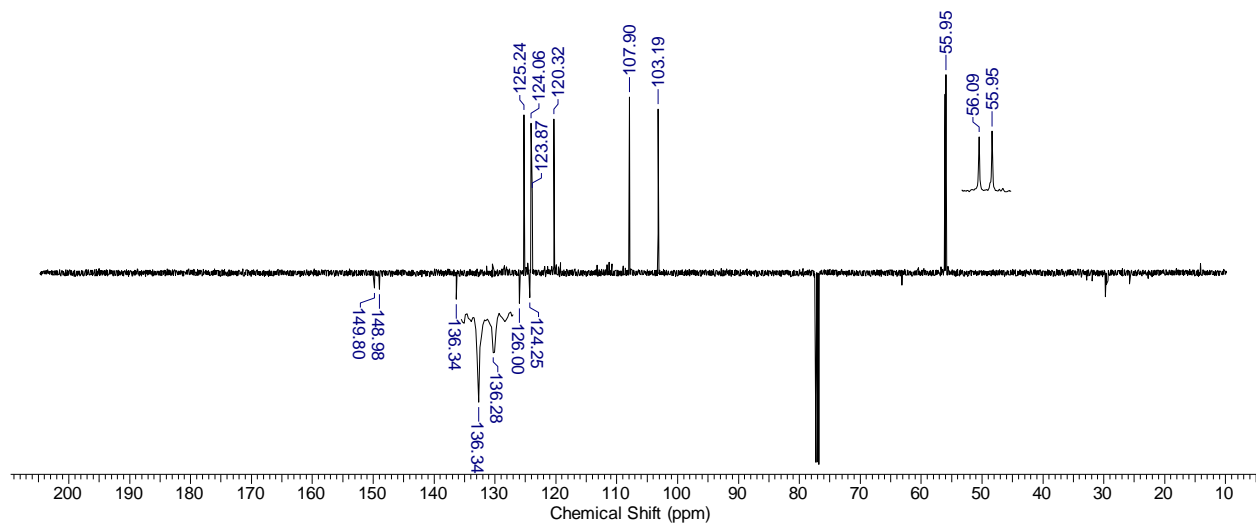


Figure S4. ¹³C NMR-spectra (DEPT) of **3b** in CDCl₃, Bruker 500 MHz.

1.2.3. Comparison of ^1H NMR of the starting **1** and its cyclization products

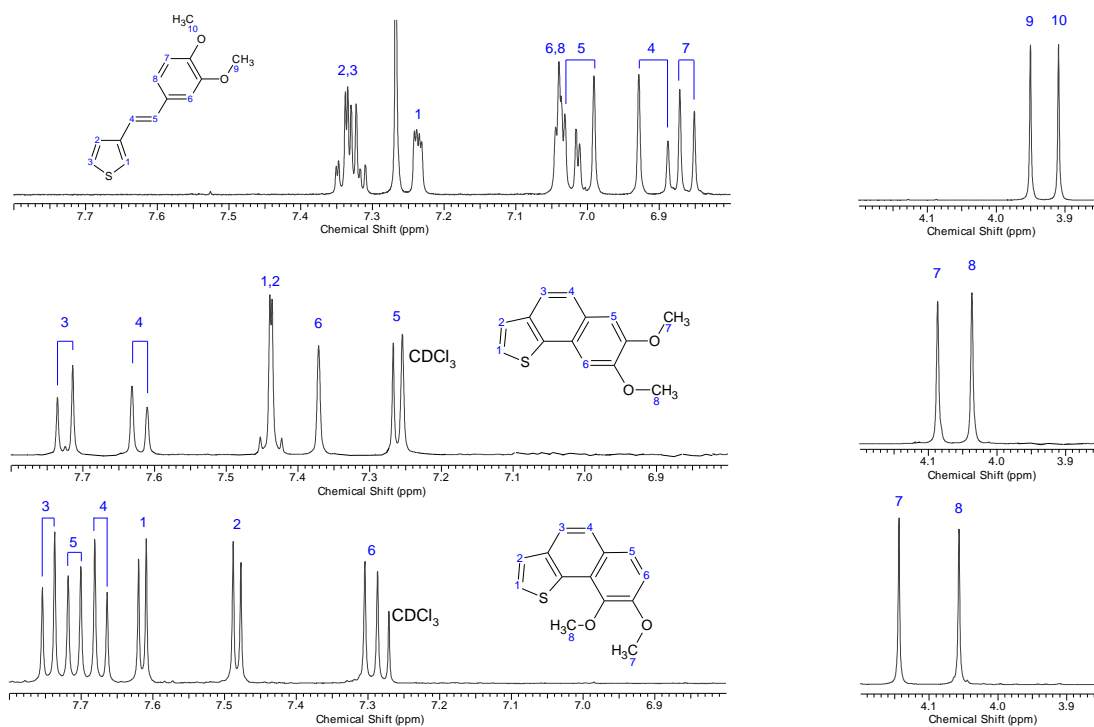


Figure S5. ^1H NMR spectra of compounds **1**, **3b**, **3a** in CDCl_3 , Bruker 400 MHz.

1.2.4. Spectra of compound 3a

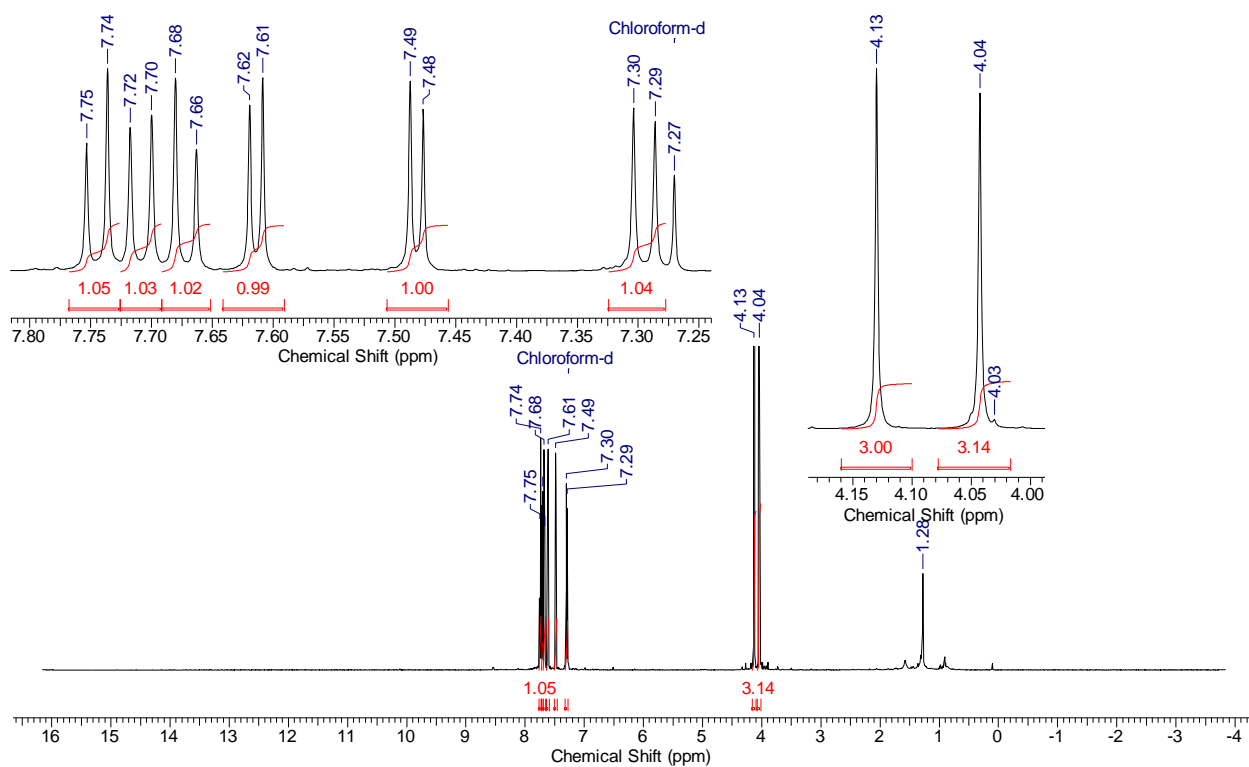


Figure S6. ^1H NMR-spectra of **3a** in CDCl_3 , Bruker 500 MHz.

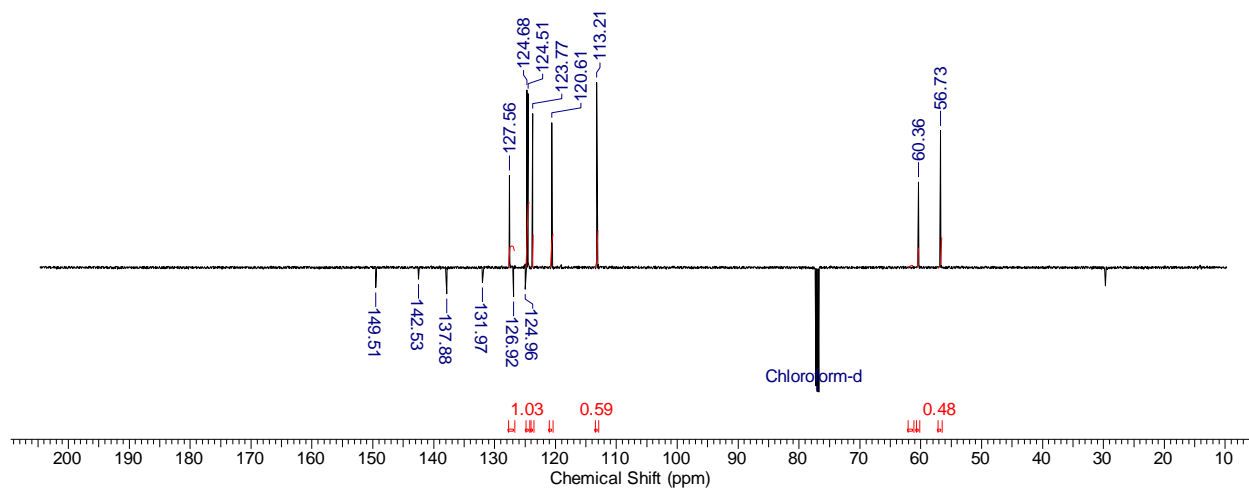


Figure S7. ^{13}C NMR-spectra of **3a** in CDCl_3 , Bruker 500 MHz.

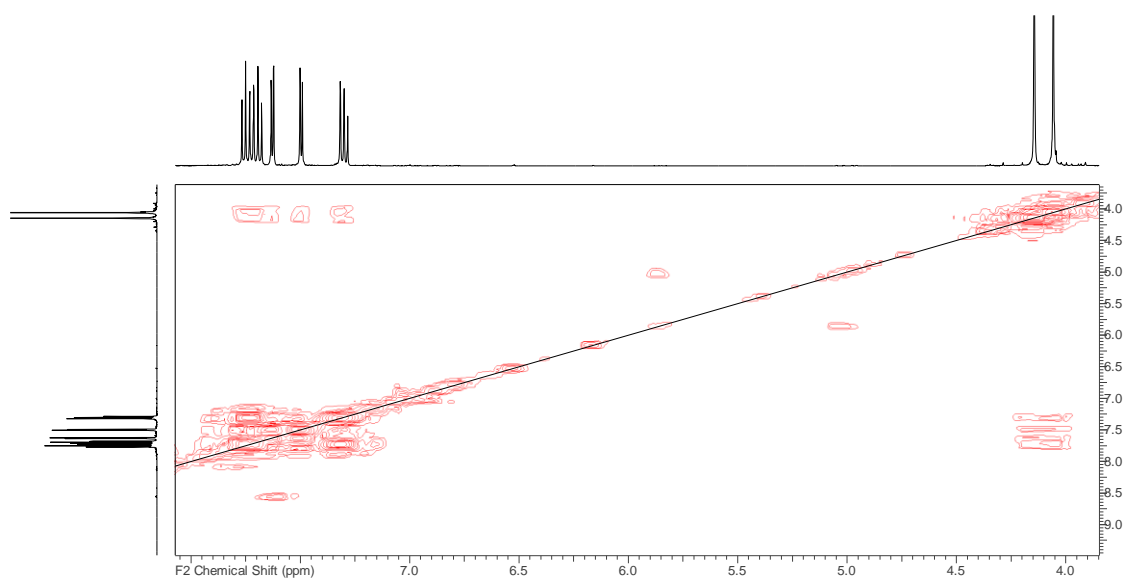


Figure S8. COSY 8,9-dimethoxynaphtho[1,2-b]thiophene (**3a**)

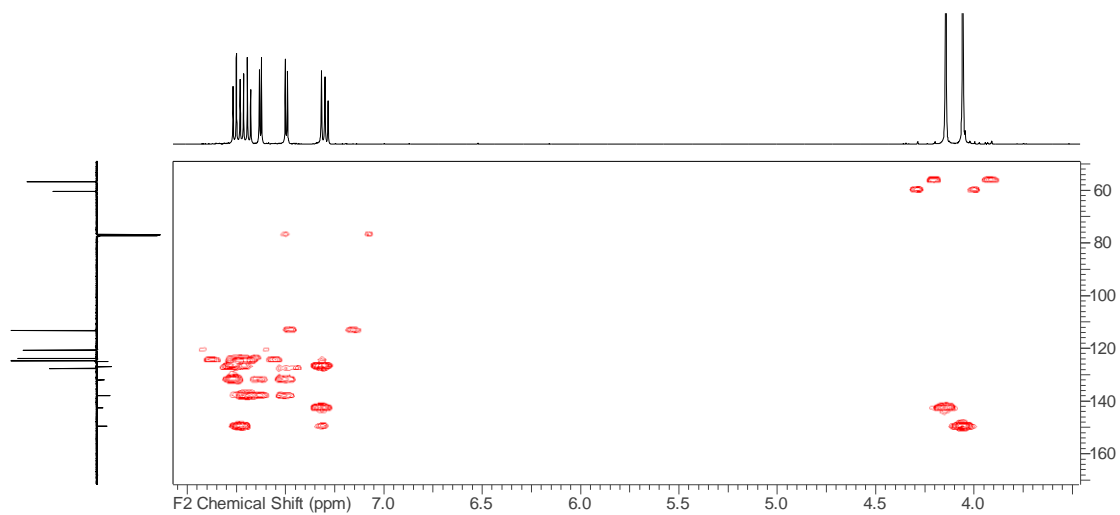


Figure S9. HMBC 8,9-dimethoxynaphtho[1,2-b]thiophene (**3a**)

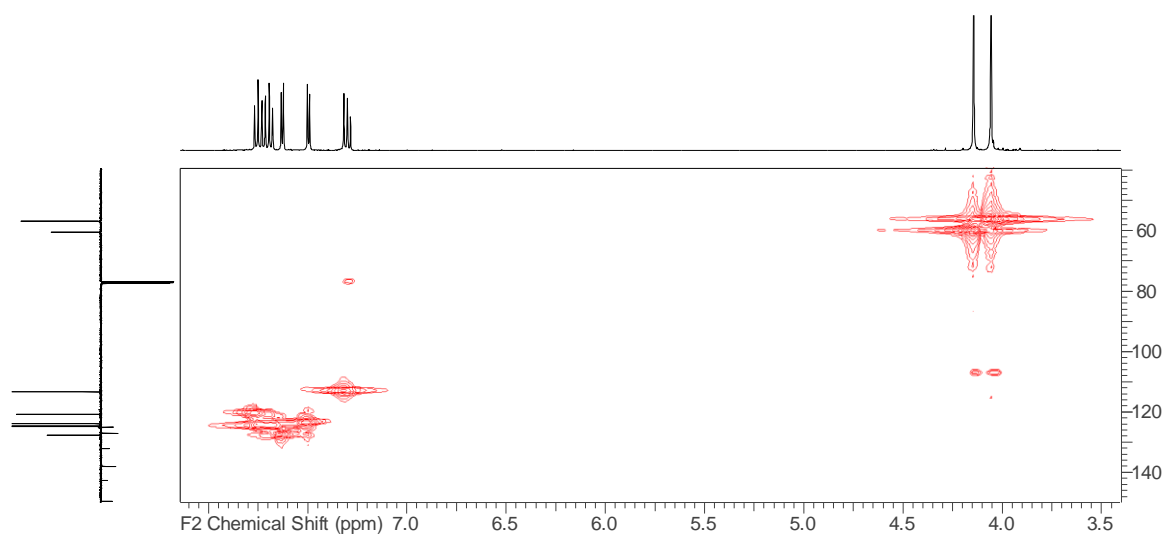


Figure S10. HMQC 8,9-dimethoxynaphtho[1,2-b]thiophene (**3a**)

1.2.5. Spectra of compound 4b

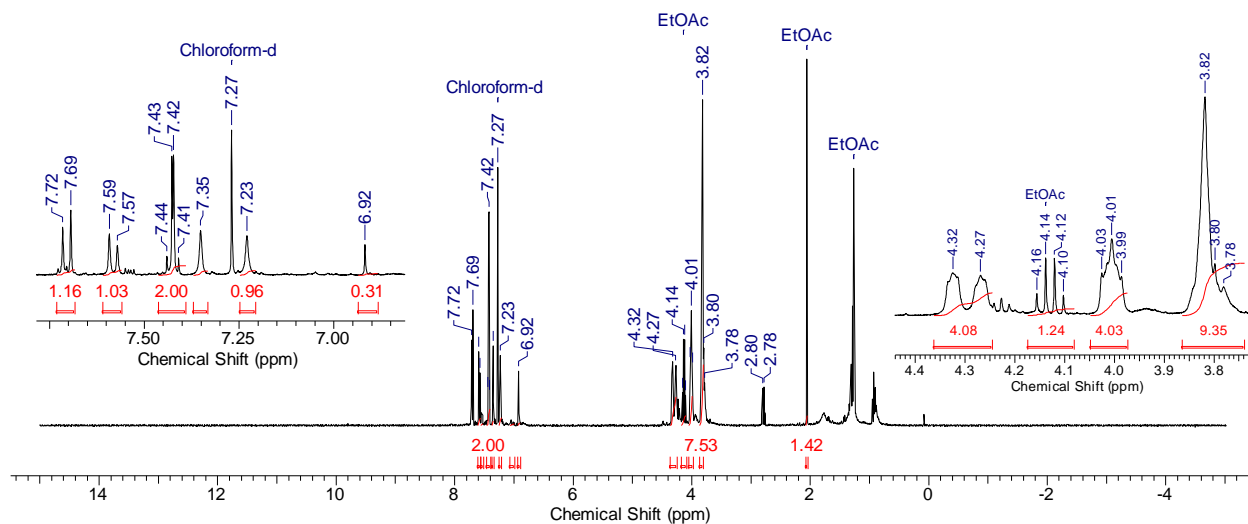


Figure S11. 8,9,11,12,14,15,17,18-Octahydrothieno[2',3':5,6]naphtho[2,3-*b*][1,4,7,10,13]penta-oxacyclopentadecine **4b**

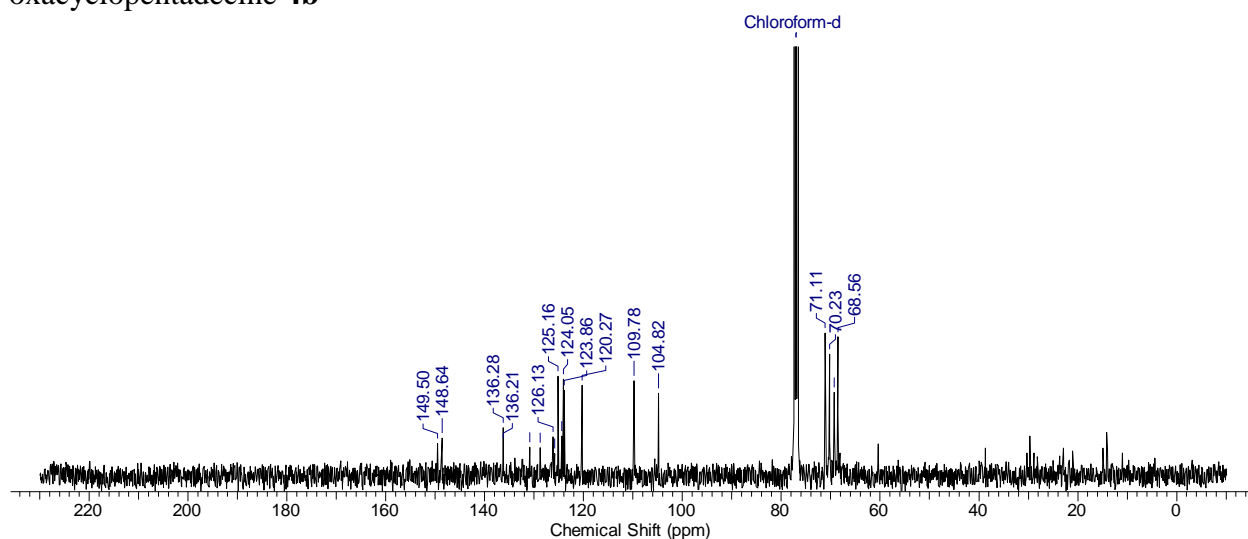


Figure S12. ^{13}C 8,9,11,12,14,15,17,18-Octahydrothieno[2',3':5,6]naphtho-[2,3-*b*][1,4,7,10,13]penta-oxacyclopentadecine **4b**

1.2.6. Spectra of compound 4a

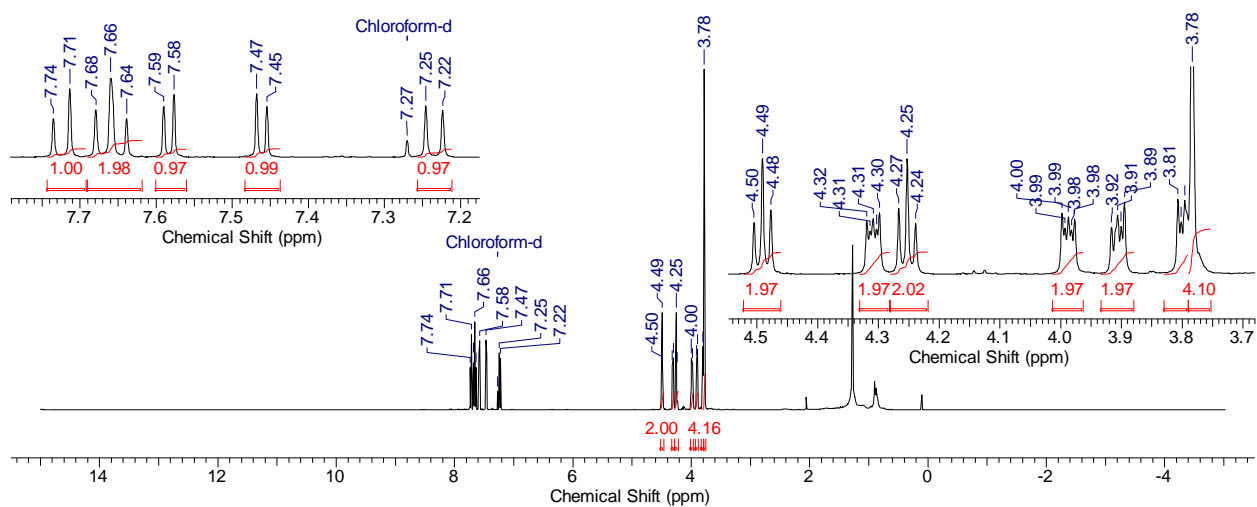


Figure S13. ^1H spectrum of 2,3,5,6,8,9,11,12-Octahydrothieno[3',2':7,8]naphtho[1,2-*b*][1,4,7,10,13]pentaoxacyclopentadecine **4a**

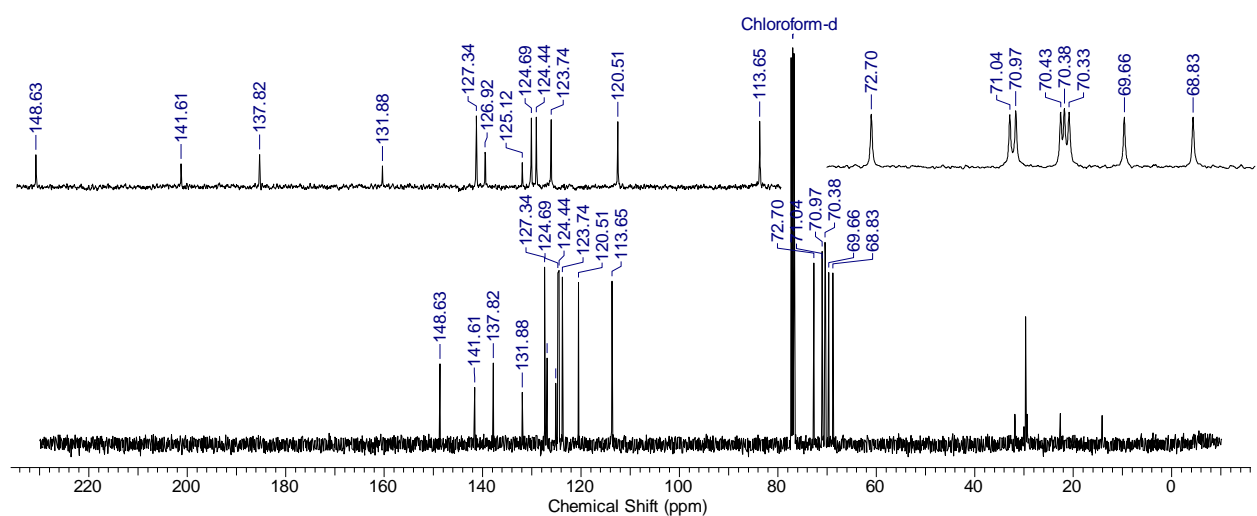


Figure S14. ^{13}C spectrum of 2,3,5,6,8,9,11,12-Octahydrothieno[3',2':7,8]naphtho[1,2-*b*][1,4,7,10,13]pentaoxacyclopentadecine **4a**

2. Photophysical properties

UV-vis and fluorescence spectroscopy measurements. UV-vis absorption spectra were recorded on a high-speed fiber optic spectrometer AvaSpec-2048-USB2, Avantes BV under continuous irradiation. The steady-state UV-vis absorption spectra were recorded on spectrophotometer Cary-300 (Agilent Technologies, USA). The fluorescence measurements were performed using a FluoroLog-3-221 spectrofluorimeter (Horiba Scientific). All measured fluorescence spectra were corrected for the non-uniformity of detector spectral sensitivity. Quinine sulfate in 1N H₂SO₄ ($\phi^{\text{fl}} = 0.55$) and rhodamine 6G in ethanol ($\phi^{\text{fl}} = 0.95$) [S3] were used as references for the fluorescence quantum yield measurements.

2.1. Absorption and emission spectra

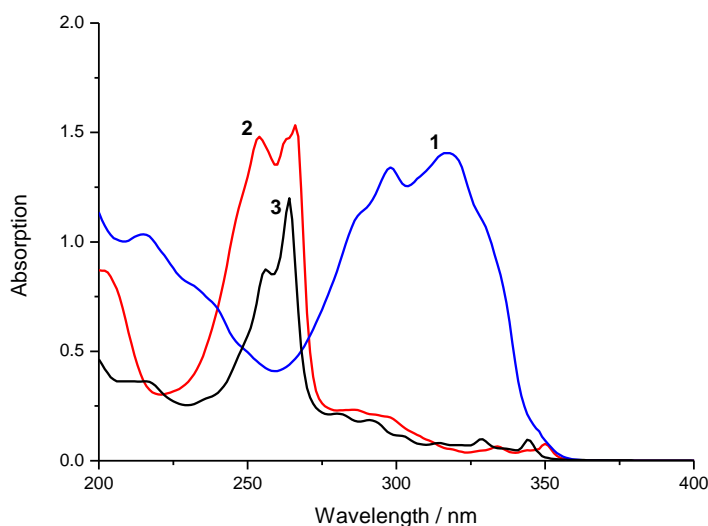


Figure S15. Electronic absorption spectra of compounds **1** (1), **3b** (2) and **3a** (3) in cyclohexane, $C=6 \times 10^{-5} M$.

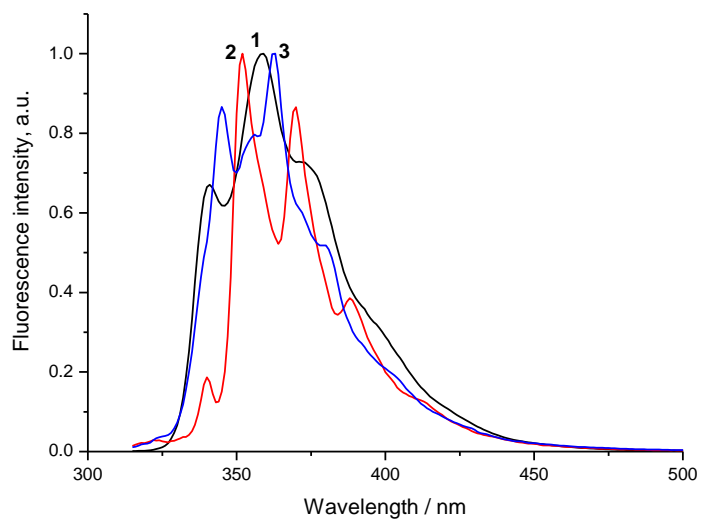


Figure S16. Normalized fluorescence emission spectra of compounds **1** (1), **3b** (2) and **3a** (3) in cyclohexane, $\lambda_{\text{ex}} = 310$ nm.

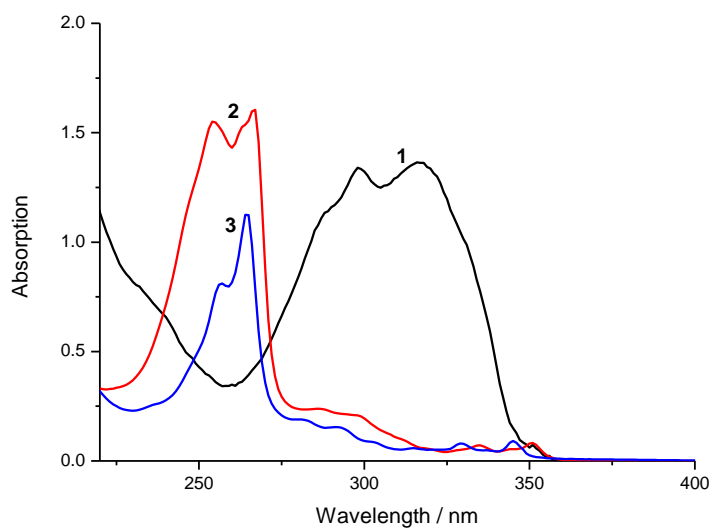


Figure S17. Electronic absorption spectra of compounds **2** (1), **4b** (2) and **4a** (3) in cyclohexane, $C=6 \times 10^{-5}$ M.

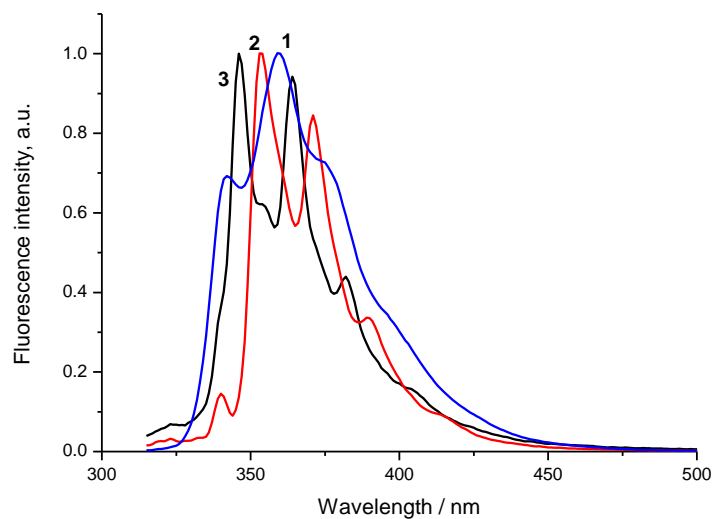


Figure S18. Normalized fluorescence emission spectra of **2** (1), **4b** (2) and **4a** (3) in cyclohexane, $\lambda_{\text{ex}} = 310$ nm.

2.2. Fluorescence decay curves

Fluorescence decay measurements were carried out using a spectrofluorometer FluoroLog-3-221 (Horiba Scientific) equipped with Time-Correlated Single Photon Counting (TCSPC) module and solid-state pulsed NanoLED emitting at 310 nm and 1 MHz pulse repetition rate. To determine fluorescence lifetimes the fluorescence kinetics were analyzed by fitting the decay curves with the use of the DAS6 program. The relative accuracy of the lifetime measurements done under the same conditions was ± 0.01 ns.

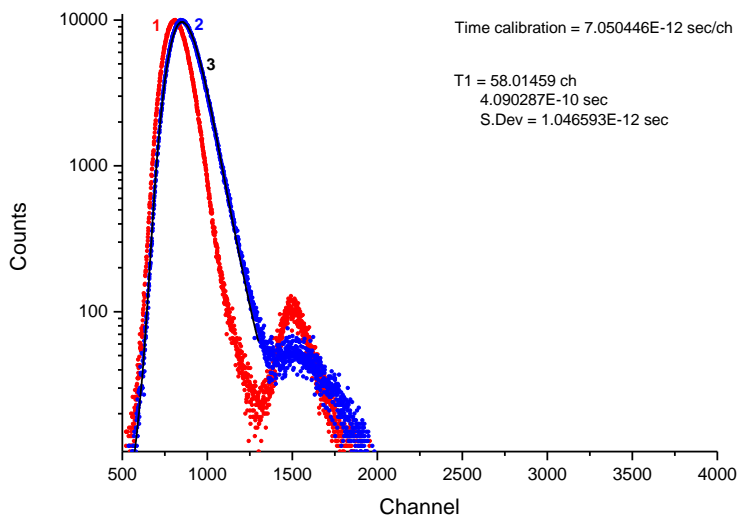


Figure S19. TCSPC histograms of instrumental response (1, red), fluorescence decay for **1** in cyclohexane (2, blue) and the best monoexponential fit of fluorescence decay (3, black) in log scale. Excitation with 310 nm NanoLED; time calibration is 7.050446×10^{-12} sec per channel. T1 is fluorescence lifetime.

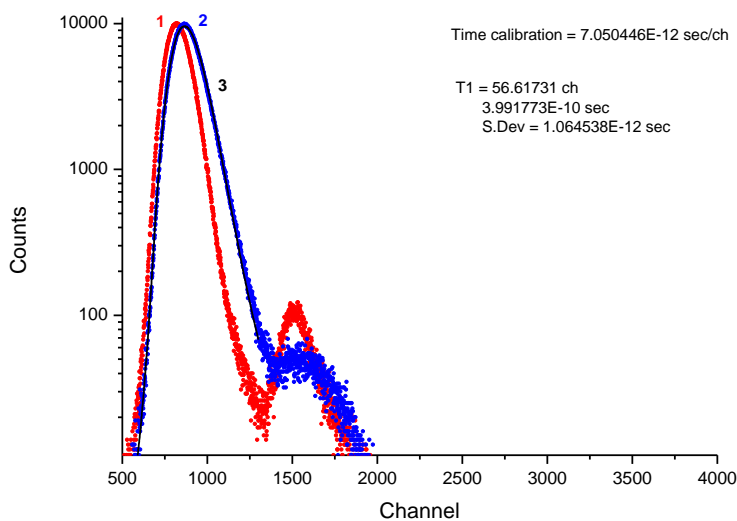


Figure S20. TCSPC histograms of instrumental response (1, red), fluorescence decay for compound **2** in cyclohexane (2, blue) and the best monoexponential fit of fluorescence decay (3, black) in log scale. Excitation with 310 nm NanoLED; time calibration is 7.050446×10^{-12} sec per channel. T1 is fluorescence lifetime.

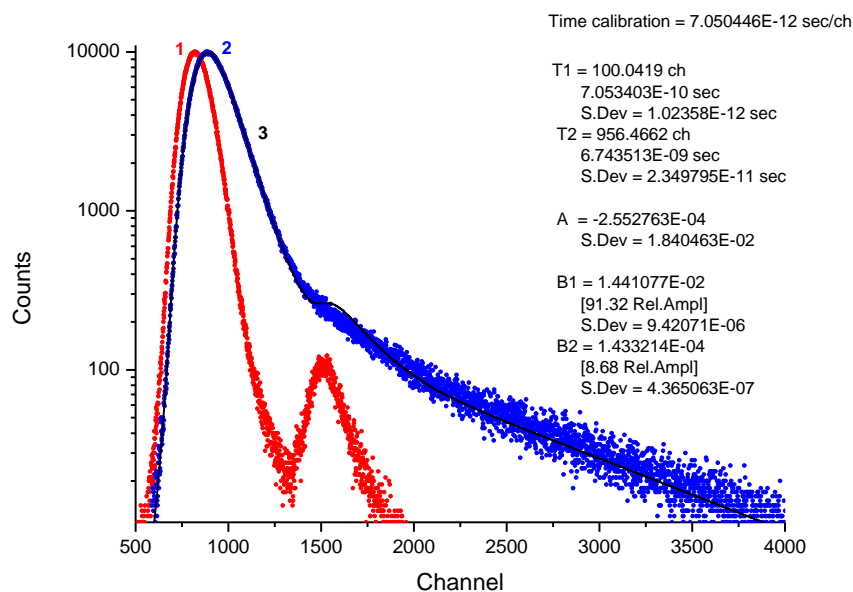


Figure S21. TCSPC histograms of instrumental response (1, red), fluorescence decay of compound **3a** in cyclohexane (2, blue) and the best biexponential fit of fluorescence decay (3, black) in log scale. Excitation with 340 nm NanoLED; time calibration is 7.050446×10^{-12} sec per channel. T1, T2 are fluorescence lifetimes.

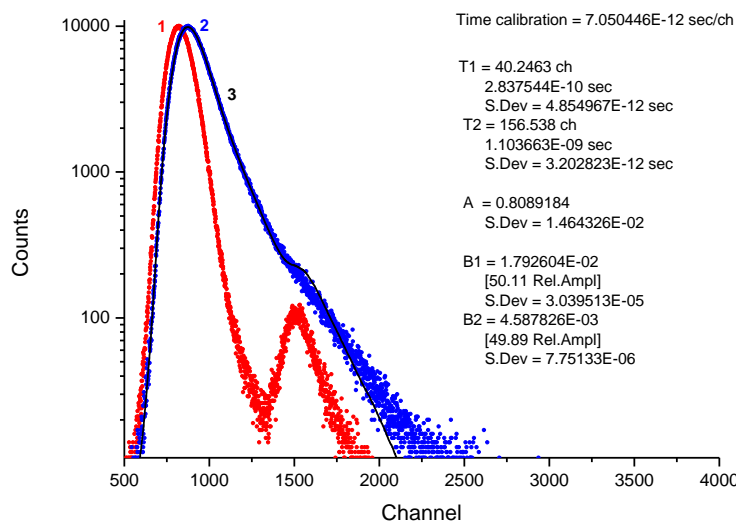


Figure S212. TCSPC histograms of instrumental response (1, red), fluorescence decay for compound **3b** in cyclohexane (2, blue) and the best biexponential fit of fluorescence decay (3, black) in log scale. Excitation with 310 nm NanoLED; time calibration is 7.050446×10^{-12} sec per channel. T1, T2 are fluorescence lifetimes.

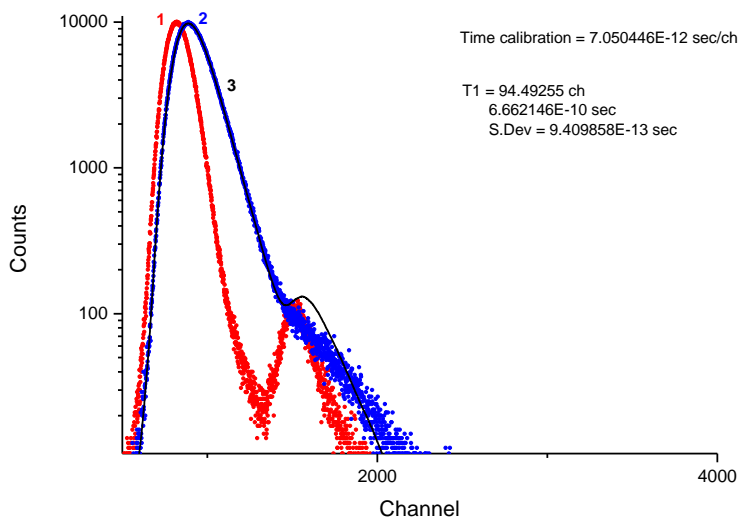


Figure S223. TCSPC histograms of instrumental response (1, red), fluorescence decay for compound **4b** in cyclohexane (2, blue) and the best monoexponential fit of fluorescence decay (3, black) in log scale. Excitation with 310 nm NanoLED; time calibration is 7.050446×10^{-12} sec per channel. T1 is fluorescence lifetime.

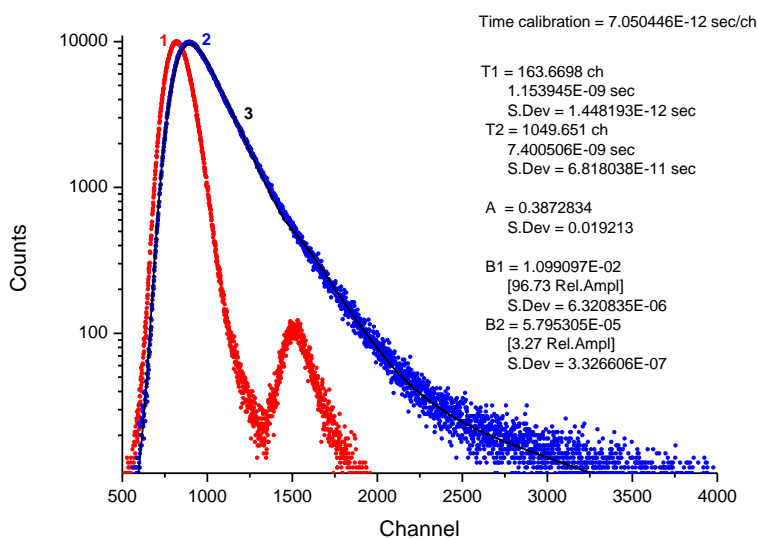


Figure S234. TCSPC histograms of instrumental response (1, red), fluorescence decay for compound **4a** in cyclohexane (2, blue) and the best biexponential fit of fluorescence decay (3, black) in log scale. Excitation with 310 nm NanoLED; time calibration is 7.050446×10^{-12} sec per channel. T1, T2 are fluorescence lifetimes.

2.3. Fluorescence quantum yield determination

All measured fluorescence spectra were corrected for nonuniformity of detector spectral sensitivity. Quinine bisulfate ($\phi_{fl} = 0.546$) was used as a reference for the fluorescence quantum yield measurements³. The fluorescence quantum yields were calculated using equation (1):

$$\phi_i = \phi_0 \left(\frac{(1-10^{-A_0}) S_i n_0^2}{(1-10^{-A_i}) S_0 n_i^2} \right) \quad (1)$$

where ϕ_i and ϕ_0 are the fluorescence quantum yields of the studied solution and the standard compound, respectively; A_i and A_0 are the absorptions of the studied solution and the standard, respectively; S_i and S_0 are the areas underneath the curves of the fluorescence spectra of the studied solution and the standard, respectively; and n_i and n_0 are the refractive indices of the solvents for the substance under study and the standard compound ($n_i = 1.42662$, cyclohexane; $n_0 = 1.339$, 1 N H₂SO₄ in water).

2.4. Quantum yields of trans-cis-isomerization

Photochemical trans-cis-isomerization was performed by irradiating of cyclohexane solutions of *E-1*, *E-2* with a filtered light of a mercury lamp (DRK-120, 120 W). The line of the mercury lamp spectrum at $\lambda = 313$ nm was separated with the use of glass filters from a standard kit of colored glass filters (UFS-2 + ZhS-3). The light intensity at $\lambda = 313$ nm was measured with the ferrioxalate actinometer and it was found to be $1.6 \cdot 10^{-6}$ Einstein s⁻¹ L⁻¹ (for experiment with *E-1*) and $1.3 \cdot 10^{-6}$ Einstein s⁻¹ L⁻¹ (for experiment with *E-2*). The photoisomerization was studied with stirring in a 1-cm quartz cuvette with a fluoroplastic stopper. Absorption spectra were recorded at regular intervals upon continuous irradiation of the sample solution using a spectrophotometer Avantes AvaSpec-2048. The time dependence of *E-1* or *E-2* absorption at $\lambda = 313$ nm upon irradiation at $\lambda = 313$ nm showed that the photostationary state is not achieved upon irradiation due to the fact that in addition to trans-cis isomerization upon irradiation, an irreversible formation of the product of photocyclization is observed. For this reason, when analyzing the kinetic curve, the possibility of the reversible reaction of trans-cis isomerization and the irreversible photocyclization reaction was taken into account. To calculate the quantum yields of all photochemical processes, the absorption spectra of all compounds formed during photolysis were measured or calculated. *Z-1*, **3a,b** and **4a,b** were isolated in a solid form from irradiated solutions of *E-1* or *E-2* by column chromatography and their absorption spectra in cyclohexane were recorded. *Z-2* was not isolated in a solid form, so its absorption spectrum was recorded in MeCN-H₂O (80%-20%) mixture after separation of irradiated solution of *E-2* by HPLC. The spectrum of *Z-2* was corrected to known concentration taking into account the absorption value at 273 nm isosbestic point observed for irradiated solution of *E-2* with known concentration in MeCN-H₂O (80%-20%). The spectra of *Z-2* in CH₃CN-H₂O (80%-20%) and in cyclohexane were considered to be identical, as it was shown that spectra of *E-2* in CH₃CN-H₂O (80%-20%) and in cyclohexane are practically identical (Figure S23).

The quantum yields of photoisomerization, $\phi(E \rightarrow Z)$ and $\phi(Z \rightarrow E)$, as well as the quantum yield of the formation of the cyclization product, $\phi(Z \rightarrow prod)$, were determined from the analysis of the dependence of the optical density on the time of irradiation using the program Sa3.3 developed by Dominique Lavabre and others (<http://pagesperso-orange.fr/cinet.chim/index.html>).

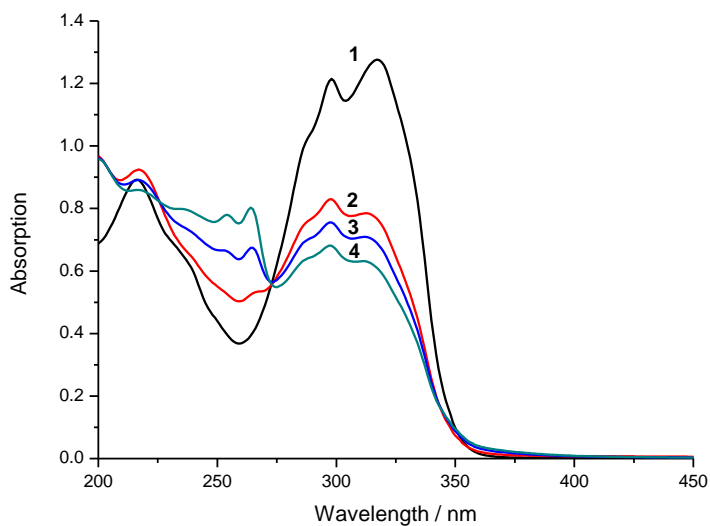


Figure S245. Dependence of electronic absorption spectra of 0.00005 M *E*-2 (1) in MeCN-H₂O (80%-20%) on irradiation time at $\lambda=254$ nm: (2) - 60 sec, (3) - 120 sec, (4) - 180 sec. Absorbance is equal to 0.5618 for isosbestic points at 273 nm.

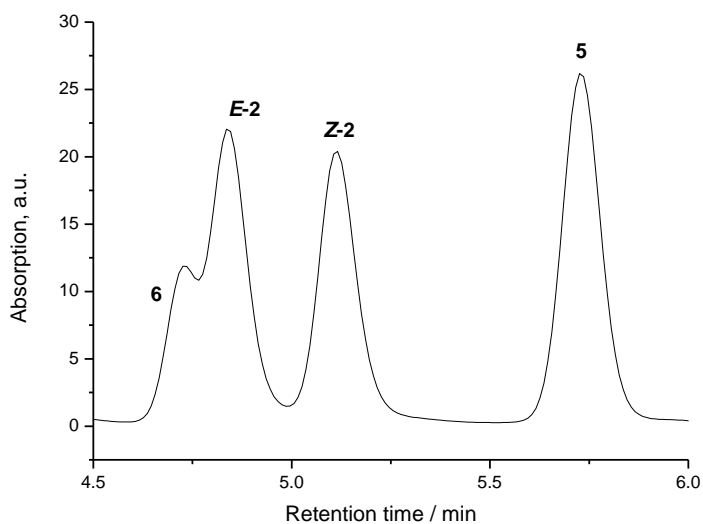


Figure S256. HPLC of the solution of *E*-2 irradiated at 254 nm for 3 min ($\lambda_{\text{mon}} = 273$ nm; [*E*-2] = 5×10^{-5} M).

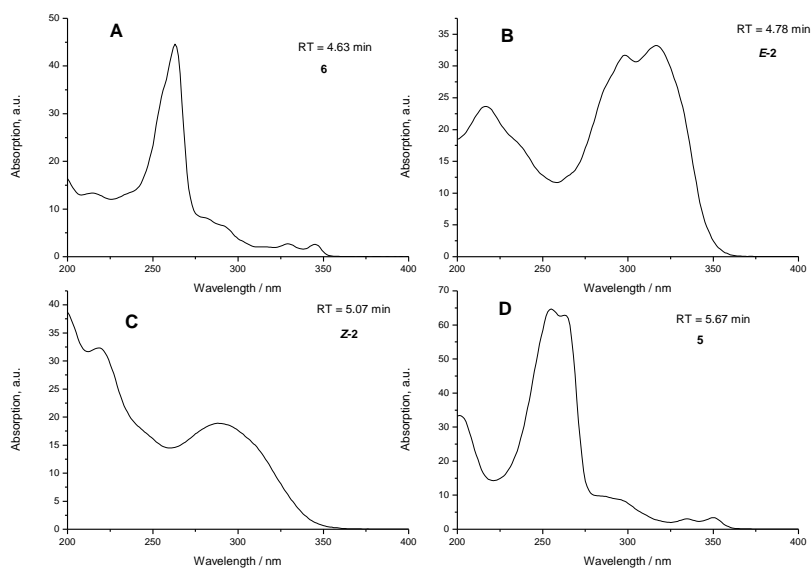


Figure S267. Electronic absorption spectra of components of irradiated solution of *E-2* separated with HPLC: (A) – **4a**, retention time 4.63 min, (B) – *E-2*, retention time 4.78 min, (C) – **Z-2**, retention time 5.07 min, (D) – **4b**, retention time 5.67 min. [*E-2*] = 5×10^{-5} M, irradiation at 254 nm for 3 min.

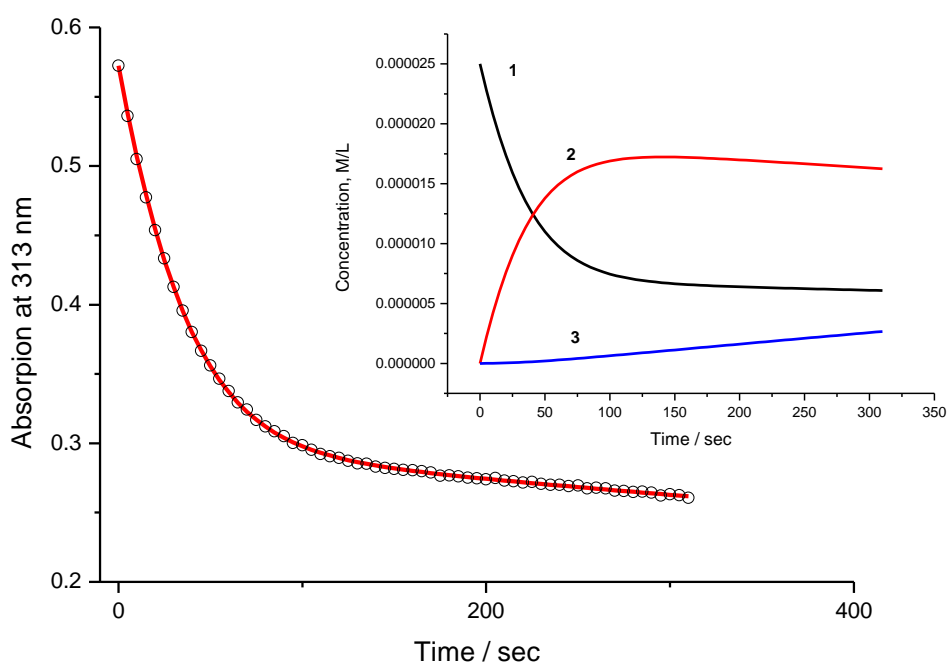


Figure S278. The time dependence of the *E-1* ($C = 2.5 \times 10^{-5}$ M) absorption at $\lambda = 313$ nm upon irradiation at $\lambda = 313$ nm (circles) and fitted curve for quantum yields $\Phi_{tr-cis} = 0.39$; $\Phi_{cis-tr} = 0.44$; $\Phi_{cis-prod} = 0.028$; and light intensity at $\lambda = 313$ nm $I = 1.6 \times 10^{-6}$ Einstein $L^{-1} s^{-1}$. Inset: the time evolution of the concentrations of *E-1* (1), *Z-1* (2) and the photoproduct **3b** (3) during the irradiation at $\lambda = 313$ nm (cyclohexane, $C = 2.5 \times 10^{-5}$ M, $I = 1.6 \times 10^{-6}$ Einstein $L^{-1} s^{-1}$, $T = 293$ K).

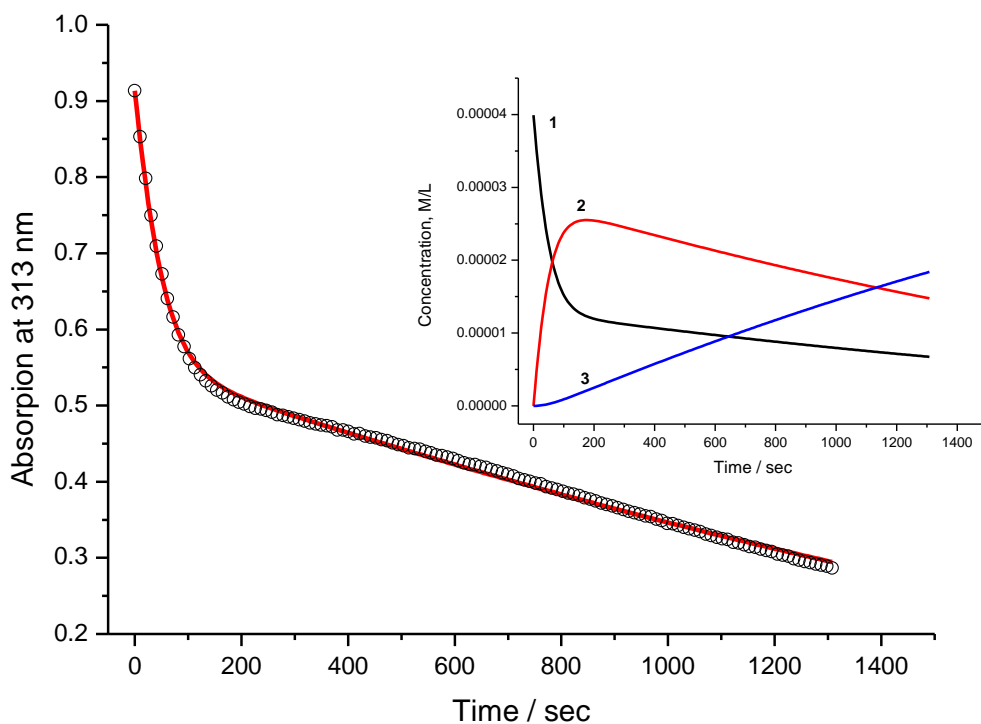


Figure S289. The time dependence of the *E*-2 ($C = 4.0 \times 10^{-5}$ M) absorption at $\lambda = 313$ nm upon irradiation at $\lambda = 313$ nm (circles) and fitted curve for quantum yields $\Phi_{\text{tr-cis}} = 0.44$; $\Phi_{\text{cis-tr}} = 0.49$; $\Phi_{\text{cis-prod}} = 0.045$; and light intensity at $\lambda = 313$ nm $I = 1.3 \times 10^{-6}$ Einstein $\text{L}^{-1} \text{s}^{-1}$. Inset: the time evolution of the concentrations of *E*-2 (1), *Z*-2 (2) and the photoproduct **3a** (3) during the irradiation at $\lambda = 313$ nm (cyclohexane, $C = 4.0 \times 10^{-5}$ M, $I = 1.2 \times 10^{-6}$ Einstein $\text{L}^{-1} \text{s}^{-1}$, $T = 293$ K).

References

- [S1] E. V. Lukovskaya, A. A. Bobyleva, O.A. Fedorova, Yu. V. Fedorov, A. V. Anisimov, Y. Didane, H. Brisset, F. Fages., *Russ. Chem. Bull.*, 2009, **58**, 1509.
 [S2] I. Moreno, I. Tellitu, E. Dominguez, Raul SanMartin, *Eur. J. Org. Chem*, 2002, 2126.
 [S3] J. R. Lakowicz, *Principles of Fluorescence Spectroscopy*, 3rd edn., Springer, Berlin, 2006.